Plasmonics (2016) 11:1067–1072
DOI 10.1007/s11468-015-0143-8

A Super Meta-Cone Absorber for Near-Infrared Wavelengths

Qiang Li[1,2] · **Jinsong Gao**[1,2] · **Haigui Yang**[2] · **Hai Liu**[2]

Received: 25 September 2015 / Accepted: 16 November 2015 / Published online: 23 November 2015

Abstract We present a meta-cone absorber based on metamaterials which can absorb nearly all incident light in the near-infrared spectrum. The absorber has an ultrahigh absorption with a broad receiving angle and independence of polarization state. This absorption enhancement can be attributed to the excitation of slow light mode and localized surface plasmon resonances (LSPR). In addition, we use slow light theory to explain why incident light with different wavelengths are trapped at different positions. We believe our work will provide a promising candidate as absorbing elements in technical applications and scientific research.

Keywords Metamaterials · Surface plasmons · Absorber · Slow light

A near-unity absorber can absorb all incident light within the working wavelength which is fundamental for microbolometer, photodetector, solar cells, or as coating material to minimize reflections from objects [1–3]. In the past, much attention has been paid to fabricate nanostructures such as nanowire [4], nanoantennas [5], nanoparticles [6], and nanohole [7] arrays and the interaction of light with these nanostructures can excite localized surface plasmon resonances (LSPR) resulting in the enhancement of absorption. In recent years, metamaterials, artificial materials with extraordinary electromagnetic properties not found in nature, have attracted a lot of attention. Many potential applications such as invisible cloaks [8], superlensing [9], negative refraction [10], and energy harvesting [11] have been achieved by tailoring the constitutive parameters of metamaterials. An important application of metamaterials is super absorber which can reduce reflection and transmission by means of impedance matching to the space and all incident energy is consumed inside the absorber [12]. Many metamaterial-based absorbers working from the microwave to the optical regime have been proposed [13–17]. Although they can achieve near-unity absorptivity, most of them are single-band, polarization-sensitive, and narrow-accepted angles, which limit their potential applications. In this work, we propose a novel meta-cone structure on silicon substrate that works on the near-infrared spectrum from 0.8 to 2.0 μm. It has an ultrahigh absorption of approximately 100 % originated from a contribution of both slow light mode and LSPR effect. This multilayer cone absorber has the superiority of broad receiving angle and independence of polarization state.

The super meta-cone absorber is shown in Fig. 1a. It consists of a periodic array of meta-cones on Au thin film with a thickness of 100 nm. Both the diameter and period (P) of meta-cones are 200 nm. The meta-cone consists of N pairs alternating layers of dielectric Si and metal Au thin films as shown in Fig. 1b. In order to achieve an absorption as high as possible in the near infrared region, Si-film thickness (t_{Si}) of 20 nm and Au-film thickness (t_{Au}) of 10 nm are chosen for impedance matching, as illustrated in Fig. 1c.

We simulated the meta-cone structure by using the finite-difference and time domain (FDTD) algorithm and obtained the absorption curves under different conditions. Figure 2a shows the near-infrared absorption in the region from 0.8 to 2.0 μm as a function of the pairs (N) of Au/Si layers. The absorption spectra were extracted by the formula of $A=1$

✉ Haigui Yang
liqiang113@mails.ucas.ac.cn

[1] University of the Chinese Academy of Sciences, Beijing 100039, China

[2] Key Laboratory of Optical System Advanced Manufacturing Technology, Changchun Institute of Optics, Fine Mechanics and Physics, Chinese Academy of Sciences, Changchun 130033, China

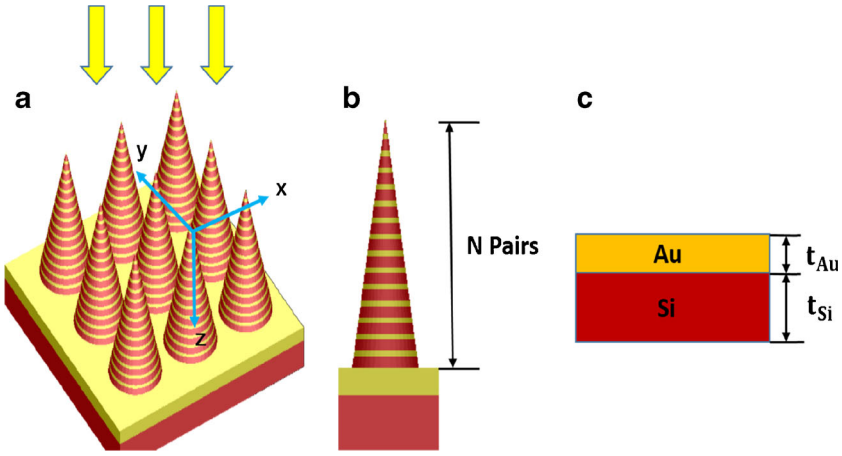

Fig. 1 **a** Schematic diagram of periodic meta-cone absorber. **b** The x–z view of one single meta-cone structure. **c** The details of one pair of the meta-cone

$-R-T$, where A is absorptance, R is reflectance, and T is transmittance. Since the thickness of bottom Au films (100 nm) is much larger than its typical skin depth, the transmission of $T=0$ was assumed in our simulation. Obviously, the designed meta-cone structure exhibits a super absorption in the near-infrared spectrum from 0.8 to 2.0 μm. In particular, at $N=60$ the average absorptance is higher than 99.5 % in the near-infrared region. Figure 2b shows the influence of filling factor (F) on the absorptance. Here, F is defined as the ratio of bottom area of a cone to the area of one unit. It is found that F has a dominant effect on the absorption in the long wavelength region. With an increase in F, the absorption becomes drastically high when the wavelength is larger than 1.5 μm. It indicates that the wavelength region with high absorption can be extended by changing F.

In addition, we studied the effect of the incident angle and polarization state of incoming light on the absorption of the meta-cone structure with $N=60$ and $F=0.75$, as shown in Fig. 2c, d. It can be seen clearly that the average absorption remains above 99.0 % for both TE and TM waves when the incident angle varies from −50° to +50°. We continued enlarging the incident angle to 70°, the absorptance dropped. However, it is still higher than 85.0 % for TM wave and 92.0 % for TE wave, which are still the highest level ever reported. This insensitivity to both incident angle and polarization state should attribute to the inherent completely symmetrical nature of the meta-cone. These simulation results in Fig. 2 prove that the cone structure designed in this study is independent of incoming light polarization state and insensitive to incident angle.

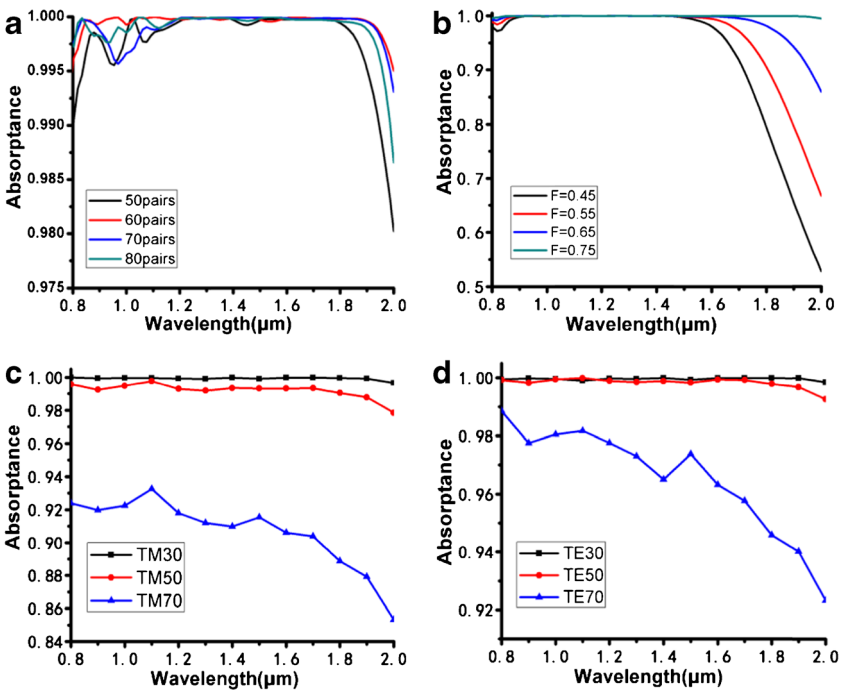

Fig. 2 **a** Under normal incident light, the absorption of meta-cone absorber as a function of the pairs (N) of Au/Si layers when $P=0.2$ μm and $F=0.75$. **b** Under normal incident light, the absorption as a function of f when $P=0.2$ μm and $N=60$. **c** and **d** represent the absorption spectra for TE and TM waves with the incident angle of 30°, 50°, and 70°

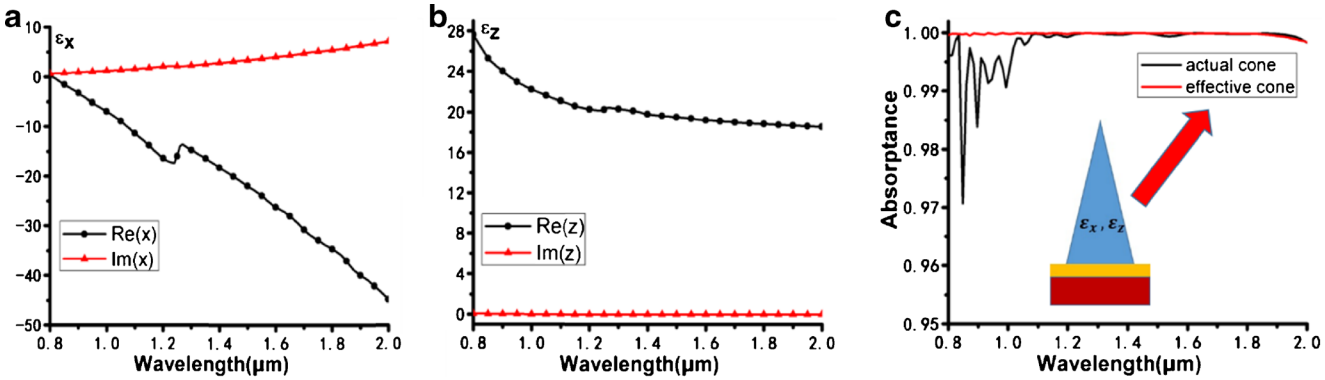

Fig. 3 **a** and **b** Calculated anisotropic permittivities of the effective medium. **c** Absorption spectrum comparison between the effective homogeneous cone structure (*red line*) and actual cone structure (*blue line*) where N=60 and F=0.75

To clarify the absorption mechanisms of the meta-cone absorber, first, we analyze this structure by the effective-medium theory [18]. According to the effective-medium theory, the Si/Au meta-cone can be considered as a homogeneous material because the thickness of both Si and Au layers is thinner enough compared with the incident

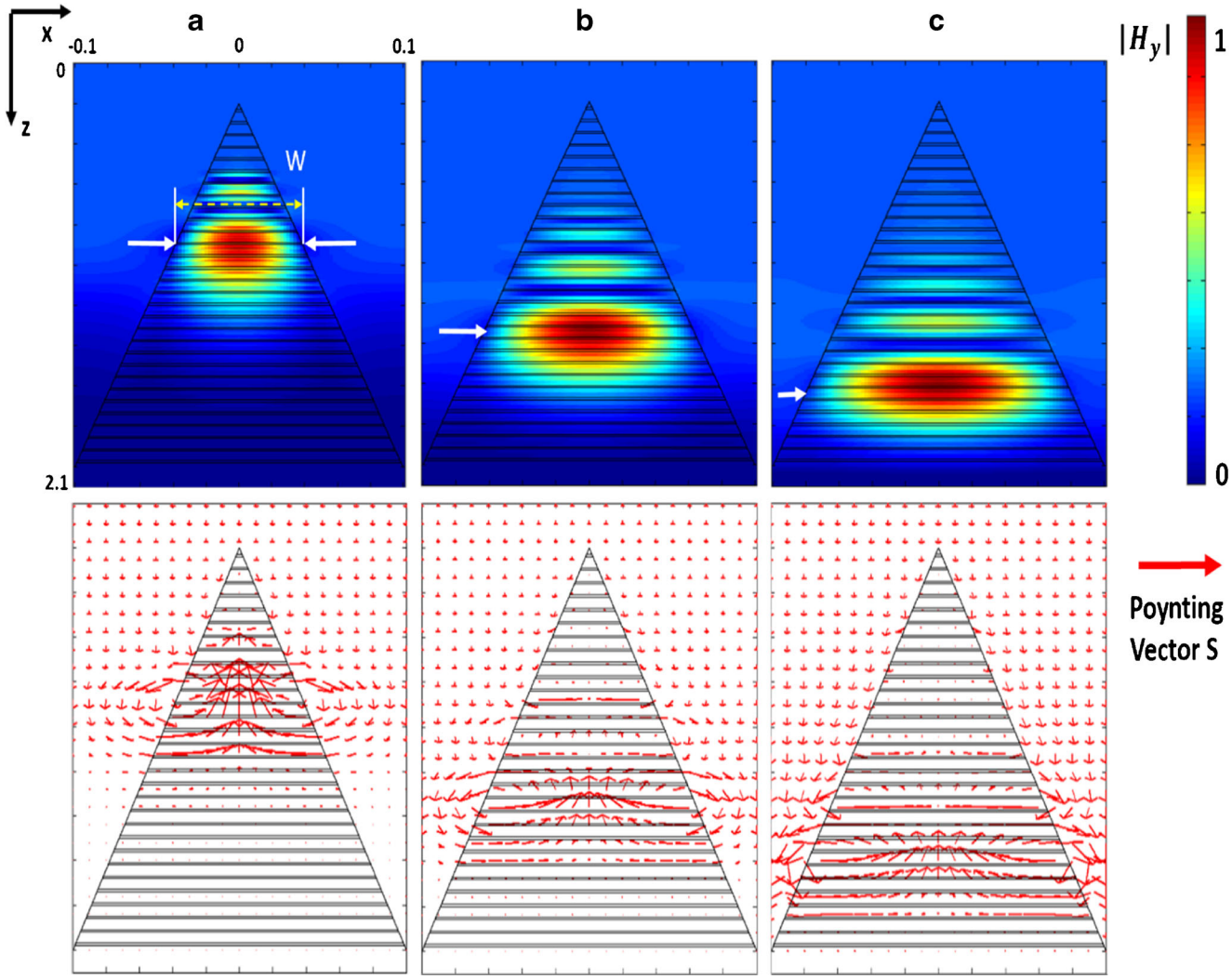

Fig. 4 Distributions of magnetic field |Hy| (top color maps) and energy flow (bottom arrow maps) for the cone absorber at different incident wavelengths: **a** 1.0 μm, **b** 1.4 μm, and **c** 1.7 μm. The maximal field position is indicated by the *white arrow* in top color maps

wavelength. In this case, the Si/Au meta-cone is regarded as a metamaterial (the inset of Fig. 3c), whose permittivity could be expressed as:

$$\varepsilon_x = \varepsilon_y = f\varepsilon_{\mathrm{Au}} + (1-f)\varepsilon_{\mathrm{Si}} \quad (1)$$

$$\frac{1}{\varepsilon_Z} = \frac{f}{\varepsilon_{\mathrm{Au}}} + \frac{1-f}{\varepsilon_{\mathrm{Si}}} \quad (2)$$

where $\varepsilon_{\mathrm{Au}}$ and $\varepsilon_{\mathrm{Si}}$ are the permittivities of Au and Si extracted from the literatures [19, 20], f is the filling ratio (1/3) of Au layers defined as $f = \frac{t_{\mathrm{Au}}}{t_{\mathrm{Au}}+t_{\mathrm{Si}}}$. Therefore, the Si/Au meta-cone can be regarded as a cone consisting of homogeneous material. The effective permittivities calculated using Eqs. (1 and 2) are shown in Fig. 3a, b, by which we obtained the absorption spectrum (red line) of the effective cone structure as shown in Fig. 3c. We found it was in good agreement with the absorptance spectrum (black line) of the actual meta-cone structure. It indicates that the effective-medium theory used in this study is valid.

In the following, we analyzed the energy flow and the y-component magnetic field (|Hy|) distribution in the plane of y=0 at the incident wavelength of 1.0, 1.4, and 1.7 μm for TM polarization wave. The simulated results are shown in Fig. 4. The plot of Poynting vector S (red arrows) describes how the incident light propagates in the meta-cone structure. At first, the incident energy propagates along z-axis before reaching the cone region, and then whirls into the cone structure from its surface. Finally, it accumulates at the position where |Hy| is enhanced greatly to the maximum, as shown in the red region of Fig. 4a. At the same time, we found an interesting phenomenon that incident light with different wavelengths was trapped at different positions of the meta-cone structure. For an example, when the wavelength of incident light is 1.0 μm, the light was trapped at an upper position of W=77.80 nm. Here, W is the width of the cone along x-axis at the white arrow in Fig. 4a. While for the light with longer wavelength of λ=1.4 μm, the energy was trapped at a lower position of W=127.80 nm. When the light wavelength further increases to 1.7 μm, it converged at a much lower position of W=150.60 nm. This indicates that the position of energy convergence is strongly dependent on light wavelength and the magnetic field around the region of energy convergence is enhanced significantly.

To explain this phenomenon, we introduced the slow light theory. Slow light means light propagates at an extremely slow group speed compared with the velocity in vacuum. In general, the group speed could be greatly reduced by a large first order dispersion arising from an optical resonance with a material or structure [21]. Many researchers have done a lot of work to realize slow light. As the reference [22] reported, a planar air waveguide with anisotropic metamaterial (AMM) cladding was proposed to slow down or even trap the light. Later, an air slab surrounded by the AMM was proved to attain zero group velocity and trap the light at different positions by carefully choosing the material parameters [23]. For our meta-cone structure, Fig. 4 shows that the light energy accumulates at the position where |Hy| is enhanced greatly to the maximum. This is a typical character for slow light mode as the Ref. [22] and [23] described, in which the light

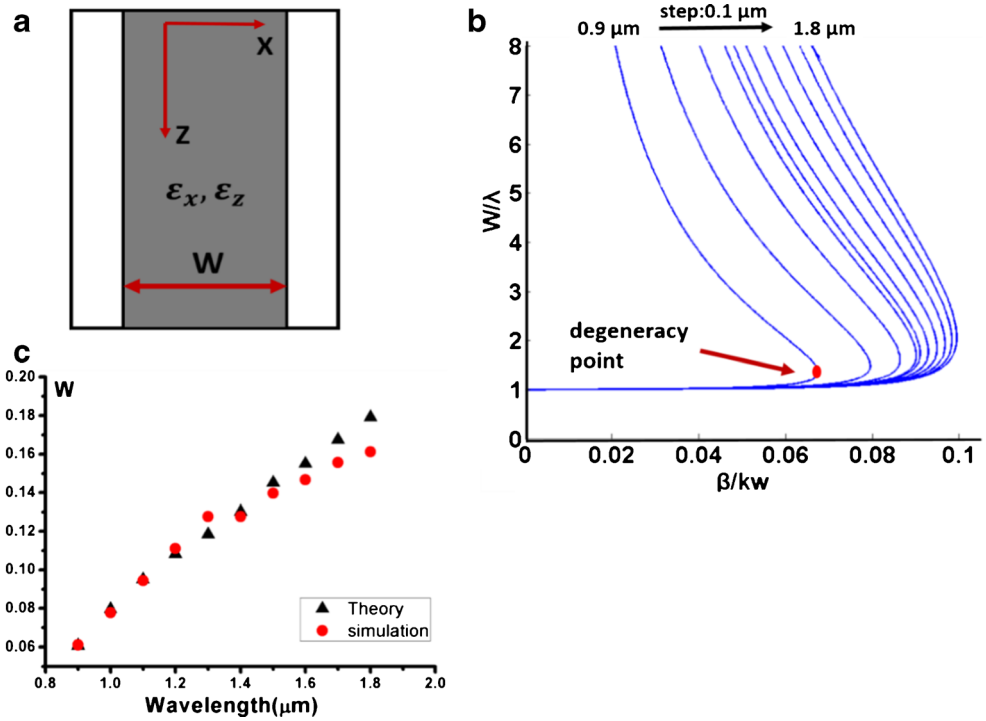

Fig. 5 **a** Diagram of an air/AMM/air waveguide with a fixed core width of W. **b** Propagation constants β of TM_0 mode as a function of the waveguide width. Two branches for each curve are separated by a degeneracy point, represented by *red circle*. The *blue lines* from left to right are respectively corresponding to the wavelengths from 0.9 to 1.8 μm with a step of 0.1 μm. We just indicate one degeneracy point and the others are similar to it. **c** Relationship between W and λ. The *black triangles* and *red solid circles* represent the W obtained by the theory of slow light mode and FDTD algorithm, respectively

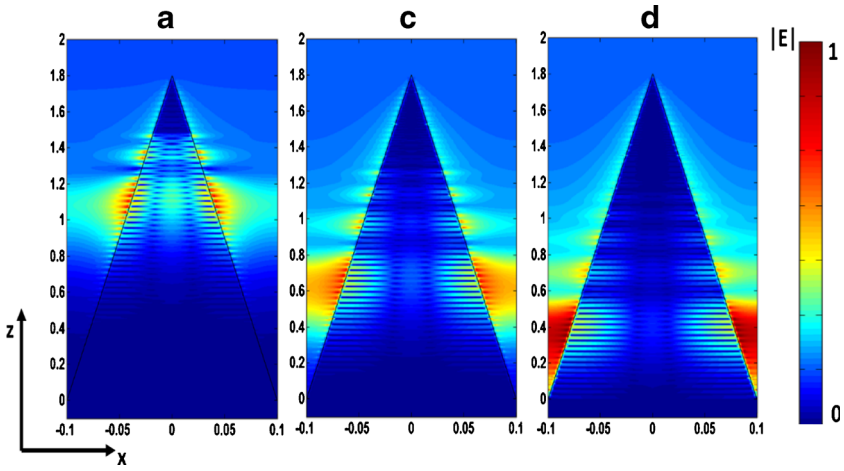

Fig. 6 Electric field |E| distributions for different wavelengths with TM polarization. **a** 1.0 μm, **b** 1.4 μm, and **c** 1.7 μm

is finally slowed down and trapped. Therefore, we can use slow light theory to explain the phenomena happened in our meta-cone structure.

Based on the analysis mentioned above, the meta-cone structure in this study could be equivalent to an air/AMM/air waveguide, as shown in Fig. 5a. The width of AMM core is W, which is the same as that in Fig. 4a. According to Maxwell function and boundary conditions, its dispersion relations can be obtained by solving the following equation [24]:

$$\tan\left(\gamma_2 \cdot \frac{W}{2}\right) = \varepsilon_z \cdot \gamma_1 \Big/ \gamma_2 \tag{3}$$

where $\gamma_1 = \left(\beta^2 - k_w^2\right)^{\frac{1}{2}}, \gamma_2 = \left(k_w^2 \cdot \varepsilon_z - \frac{\varepsilon_z}{\varepsilon_x} \cdot \beta^2\right)^{\frac{1}{2}}. k_w = \frac{w}{c}$ is the vacuum wave vector. Here, we just considered the lossless case and extracted the permittivities from 0.9 to 1.8 μm with a 0.1 μm interval by solving Eqs. (1 and 2). Using these permittivities, we achieved the dispersion curves of $\frac{\beta}{k_w}$ versus $\frac{W}{\lambda}$ of TM_0 mode by solving Eq. (3), as plotted in Fig. 5b. It can be seen clearly from Fig. 5b that AMM core layer can support two different propagation constants for each TM mode if its width is fixed. The red circle indicates the "degeneracy point" where the group speed reduces to zero resulting in the light energy trapped at this position [24]. From the x-axis value of the degeneracy point, we calculated W. For an example, when the incident wavelengths are 1.0, 1.4, and 1.7 μm, the width values are W_1= 0.0796×1 μm=79.60 nm, W_2=0.0930×1.4 μm=130.20 nm, and W_3=0.0985×1.7 μm=167.45 nm, which are in accordance with the extracted W (77.80, 127.80, and 155.60 nm) from Fig. 4. This reflects that the meta-cone structure in this study supports slow light mode which has a strong light trapped effect. Additionally, the slow light mode results in that certain wavelengths of light can be trapped at the different positions of the meta-cone structure. We use the same method mentioned above to obtain the relationship (black triangles) between W and photon wavelength in theory as shown in Fig. 5c. For a comparison, W (red circles) extracted from the |Hy| distributions are also given. Obviously, the calculated results obtained by the theory of slow light mode agree perfectly with the simulation by FDTD algorithm. Therefore, by this theory, we can explain well why different incident wavelengths trapped at different positions. In particular, using this theory, we can create a new approach to design an AMM core with different metal/dielectric, filling ratio f, and width W so that the absorption spectrum can be tuned. That is the nature of metamaterials, and our work is helpful in designing super absorber in the near infrared region.

In addition, the distributions of electric field (|E|) at various incident wavelengths with TM polarization were also simulated. It is obvious from Fig. 6 that |E| is enhanced greatly at both edges of the meta-cone structure, especially at the interface between Au/Si layers. |E| enhancement can be attributed to the LSPR enhancement effect in Au/Si composites. Our simulation result is in accordance with the characteristic of LSPR. As a result, LSPR can enhance the absorption of incident energy and it is considered as another reason to enhance the near-infrared absorption.

In conclusion, we have successfully demonstrated a near-infrared absorber based on metamaterials, which has an ultrahigh absorption of 99.5 % on average in the spectrum of 0.8–2.0 μm. It exhibits an insensitive behavior to the polarization state and keeps an ultrahigh absorption even at the incident angle as large as 70°. According to the waveguide theory, our meta-cone structure absorbs light because each cone acts as a waveguide to trap incident energy. Further, we proposed an approach which can control the position where the incident energy trapped by altering the materials or adjusting the filling ratio. And we also found the enhanced absorption was attributed to slow light mode as well as LSPR effect. This work provides a promising way to effectively enhance the near-infrared absorption of absorber. It will provide a good candidate to

design a high-performance absorber used in technical applications and scientific research.

Acknowledgments Project supported by the National Natural Science Foundation of China (Nos. 61306125 and U1435210), the Science and Technology Innovation Project (Y3CX1SS143) of CIOMP, the Science and Technology Innovation Project of Jilin Province (Nos. Y3293UM130, 20130522147JH, and 20140101176JC).

References

1. Liu XL, Starr T, Starr AF, Padilla WJ (2010) Infrared spatial and frequency selective metamaterial with near unity absorbance. Phys Rev Lett 104(20):207403
2. Landy N, Bingham C, Tyler T, Jokerst N, Smith D, Padilla W (2009) Design, theory, and measurement of a polarization-insensitive absorber for terahertz imaging. Phys Rev B 79(12): 125104
3. Diem M, Koschny T, Soukoulis CM (2009) Wide-angle perfect absorber/thermal emitter in the terahertz regime. Phys Rev B 79(3):033101
4. Zhu J, Yu Z, Burkhard GF, Hsu C-M, Connor ST, Xu Y, Wang Q, Fan S, Cui Y (2009) Optical absorption enhancement in amorphous silicon nanowire and nanocone arrays. Nano Lett 10:1021
5. Chalabi H, Schoen D, Brongersma ML (2014) Hot-electron photodetection with a plasmonic nanostripe antenna. Nano Lett 14:1374–1380
6. Yen-Hsun S, Ke Y-F, Cai S-l, Yao Q-Y (2012) Surface plasmon resonance of layer-by-layer gold nanoparticles induced photoelectric current in environmentally-friendly plasmon-sensitized solar cell. Light Sci Appl 10:1038
7. Te Lin K, Chen H-L, Lai Y-S, Yu C-C (2014) Silicon-based broadband antenna for high responsivity and polarization-insensitive photodetection at telecommunication wavelengths. Nat Commun 5:3288
8. Schurig D, Mock J, Justice B, Cummer S, Pendry J, Starr A, Smith D (2006) Metamaterial electromagnetic cloak at microwave frequencies. Science 314:5801
9. Pendry J (2000) Negative refraction makes a perfect lens. Phys Rev Lett 85:3966
10. Fok L, Zhang X (2011) Negative acoustic index metamaterial. Phys Rev B 83:214304
11. Almoneefand TS, Ramahi OM (2015) Metamaterial electromagnetic energy harvester with near unity efficiency. Appl Phys Lett 106: 153902
12. Shen X, Cui TJ, Zhao J, Ma HF, Jiang WX, Li H (2011) Polarization-independent wide-angle triple-band metamaterial absorber. Opt Express 19:009401
13. Wang B-X, Wang G-Z, Wang L-L (2015) Design of a novel dual-band terahertz metamaterial absorber. Plasmonics 14:114012
14. Dong X, Tao K, Wang Q (2015) Ultrabroadband mid-infrared light absorption based on a multi-cavity plasmonic metamaterial array. Plasmonics 10:1007
15. Grześkiewicz B, Sierakowski A, Marczewski J, Pałka N, Wolarz E (2014) Polarization-insensitive metamaterial absorber of selective response in terahertz frequency range. J Opt 16:105104
16. Sun C, Su J, Wang X (2015) A design of thin film silicon solar cells based on silver nanoparticle arrays. Plasmonics 10:1007
17. Cao S, YU W, Wang T, Xu Z, Wang C, Fu Y, Liu Y (2013) Two-dimensional subwavelength meta-nanopillar array for efficient visible light absorption. Appl Phys Lett 102:161109
18. TC Choy (1999) Effective medium theory: principles and applications. Oxford University Press on Demand 102
19. Johnson PB, Christy RW (1972) Optical constants of the noble metals. Phys Rev B 6:4370
20. ED Palik (1998) Handbook of optical constants of solids. Academic press
21. Baba T (2008) Slow light in photonic crystal. Nat Photonics 2:146
22. T Jiang, YJ Feng (2008) In: Proceedings of the International Conference on Microwave and Millimeter Wave Technology
23. Jiang T, Zhao J, Feng Y (2009) Stopping light by an air waveguide with anisotropic metamaterial cladding. Opt Express 19:170–177
24. Hu H, Ji D, Xie Z, Liu K, Gan Q (2013) Rainbow trapping in hyperbolic metamaterial waveguide. Sci Rep 3:1249